International Journal of Chemical, Materials and Biomolecular Sciences
ISSN: 2415-6620
Vol:9, No:2, 2015

Photoluminescence Study of Erbium-Mixed Alkylated Silicon Nanocrystals

Khamael M. Abualnaja, Lidija Šiller, Benjamin R. Horrocks

***Abstract*—**Alkylated silicon nanocrystals (C_{11}-SiNCs) were prepared successfully by galvanostatic etching of p-Si(100) wafers followed by a thermal hydrosilation reaction of 1-undecene in refluxing toluene in order to extract C_{11}-SiNCs from porous silicon. Erbium trichloride was added to alkylated SiNCs using a simple mixing chemical route. To the best of our knowledge, this is the first investigation on mixing SiNCs with erbium ions (III) by this chemical method. The chemical characterization of C_{11}-SiNCs and their mixtures with Er^{3+}(Er/C_{11}-SiNCs) were carried out using X-ray photoemission spectroscopy (XPS). The optical properties of C_{11}-SiNCs and their mixtures with Er^{3+} were investigated using Raman spectroscopy and photoluminescence (PL). The erbium mixed alkylated SiNCs shows an orange PL emission peak at around 595 nm that originates from radiative recombination of Si. Er/C_{11}-SiNCs mixture also exhibits a weak PL emission peak at 1536 nm that originates from the intra-4*f* transition in erbium ions (Er^{3+}). The PL peak of Si in Er/C_{11}-SiNCs mixture is increased in the intensity up to three times as compared to pure C_{11}-SiNCs. The collected data suggest that this chemical mixing route leads instead to a transfer of energy from erbium ions to alkylated SiNCs.

***Keywords*—**Photoluminescence, Silicon Nanocrystals, Erbium, Raman Spectroscopy.

I. Introduction

THE major component in microelectronic and optical communication system is silicon. There are three limitations that are associated with silicon related to their use in optical communication system i.e. Si is an indirect band gap, strong non radiative recombination pathways resulting in a very short non radiative lifetime and there is a mismatch between the band edge luminescence at 1.1 μm (1.1 eV) and the wavelength of 1.55 μm (0.8 eV) that is a requirement for compatibility with optical communication system [1]. This number of factors makes this element a poor light emitter.

The limitation of the spectral mismatch is overcome by incorporating silicon with rare earth ions such as Er, Yb, Nd and Tm. Rare earth ions emission has been widely investigated in silicon last two decade [1]-[3]. Erbium ions especially have played a crucial role in the improvement of optical communication system, due to its luminescence band being at 1.54 μm, which is the requirement in this technology. Erbium is 11th element in the series of rare earth elements which located in the sixth row of the periodic table and the electronic configuration of Er is $[Xe]4f^{12}6s^2$. It is known that Er presents intense narrow luminescence bands in both visible and near infrared regions [4]. The erbium has two oxidation states i.e. Er^{2+} and Er^{3+}, out of which the former one is very commonly seen in semiconductors; due to its radiative transition at around 1.54 μm which corresponds to the most interesting wavelength in photonics community. Losing one electron of 4f orbital and both of 6s orbital produces the trivalent erbium (Er^{3+}); thus in this ion the incomplete 4f orbital is shielded by 5s and 5p orbitals resulting in luminescence dependent host. The radiative transition of Er^{3+} in solid hosts looks like the free ion but with some changes due to Stark splitting [5].

The labels of the energy levels in rare earth ions e.g. $^4I_{13/2}$ or $^4S_{3/2}$ correspond to their angular momentum and spin quantum numbers [5]. The letters here are attributed to the total orbital angular momentum of the ion. The total orbital angular momentum is resulted by adding the orbital angular momenta of the individual electrons in the ion following the Clebsch-Gordan series [6]. Thus, the letter S indicates the orbital angular momentum (L) of 0, P of 1, D of 2, F of 3 and etc. Therefore, the letter I presents an L of 6. The superscript number 4 denotes the possible orientation of the total spin angular momentum of the ion, which is given as $2S+1$, where S is attributed to quantum numbers of spin. While the subscript presents the total angular momentum of the ion. Consequently, in rare earth ions, it should be considered that each discrete energy level is attributed to $^{2S+1}L_J$ [5].

The emission from trivalent erbium at 1554 nm (due to $^4I_{13/2}\rightarrow{}^4I_{15/2}$ transition in erbium) is a standard wavelength in the optical telecommunication system; thus it is important to achieve maximum enhancement in Er emission intensity i.e. long luminescent lifetime and high active concentration of erbium [7]. Recently, the investigation on enhancing the optical activity of erbium ions has been extensively reported [1], [8], [9]. The erbium emission can be increased by i) adding clusters which act as sensitizers for erbium excitation, ii) increasing the fraction of trivalent erbium by changing the local atomic environment and iii) optimizing the rate of erbium excitation by applying local field enhancement in presence of metallic particles [8]. The sensitization effect has recently become attractive subject because of the successful enhancement in erbium emission via range of sensitizers (host materials) including SiNCs, SiO_2 and Yb ions [7], [9]-[11].

Among the host materials, Si has received particular interest since the discovery of 1.54 μm light emission in erbium doped silicon at 20 K in 1983 by Ennen and co-workers [12] and

K. M. Abualnaja is with the School of Chemical Engineering and Advanced Materials, Newcastle University, Newcastle Upon Tyne, UK (corresponding author: +44 (0) 191 208 5619; e-mail: k.abualnaja@ncl.ac.uk).
L. Šiller is with the School of Chemical Engineering and Advanced Materials, Newcastle University, Newcastle Upon Tyne, UK (e-mail: lidija.siller@ncl.ac.uk).
B. R. Horrocksis with the School of Chemistry, Newcastle University, Newcastle Upon Tyne, UK (e-mail: ben.horrocks@ncl.ac.uk).

later they observed electroluminescence at 77 K in 1985 [13]. This effective light emission from silicon-based erbium (with sufficient high concentrations of Er) has led to a novel Si-based optoelectronics and light emitting diodes (LEDs) [14]. Taking into account the importance of 1.54 μm light emission from erbium doped silicon in optical telecommunication system, the mechanism of the energy transfer from Si to erbium has been explained as follow [1]. Generally, the mechanism of the erbium emission of erbium doped silicon is described as followed [1]. Firstly, exciton (electron-hole pair) is generated inside SiNCs by using an excitation source. Then, the exciton recombines radiatively, which causes photon emission as the energy of the resulted photon depends on the size of Si nanocrystal. A part of radiative recombination energy of the exciton of SiNCs is transferred to 4f shell in trivalent erbium; thus exciting Er^{3+}. The emission of erbium at 1.54 μm then occurs as a result of the transition from $^4I_{13/2}$ to the ground sate $^4I_{15/2}$. It is also should be noted that the amount of the energy transferred to Er^{3+} depends strongly on the concentration of erbium in the host material and the distance between Si nanocrystals and trivalent erbium as observed by [9], [15]-[17].

There are several successful techniques that used to incorporate and to produce optically active erbium ions into SiNCs including molecular beam epitaxy [18], sputtering [16], chemical vapor deposition [15], thermal diffusion[19] and ion implantation [20].

Fujii et al. [21], [22] observed that Er-doped SiNCs films exhibit two emission bands i.e. 0.81 and 1.54 μm that associated to radiative recombination inside Si nanocrystals and to intra-4f transition ($^4I_{13/2}\rightarrow{}^4I_{15/2}$) in erbium ions, respectively. They studied the correlation between the intensities of the two-luminescence bands as a function of erbium concentration. They found that the intensity of erbium emission band at 1.54 μm increased as the concentration of erbium increased, whereas the intensity of 0.81 μm decreased significantly. They suggested that the energy is transferred from Si nanocrystals to erbium ions. In contrast, [15], [16] found that the intensity of the emission peak of erbium increased with decreasing the erbium concentration. This provides also a clear evidence for the energy transfer from silicon to erbium. Also, they suggested that the intensity of this peak mainly depends on the chemical composition of the matrix where SiNCs are embedded in. However, Fujii et al. [21], [22] and Cerqueira et al. [15], [16] both observed that the PL peak of erbium ions was also more intense with small size of SiNCs embedded in silicon matrix.

John et al. [23] and Ji et al. [24] implanted Er^{3+} alongside SiNCs into SiO_2 films, where the SiNCs play as a sensitizer which absorb more photons efficiently. Thus, this leads to a significant improvement in the emission properties of Er ions as the erbium ions covalently bonded with SiNCs. In their work, Er-doped SiNCs samples exhibit NIR light emission, which created by transfer energy from Si nanocrystal to erbium. John and co-workers [23] prepared erbium doped SiNCs by the co-pyrolysis of disilane where $Er(tmhd)_3$ (tmhd = 2,2,6,6-tetramethyl1-3,5-heptanedionato) was used as a source of erbium ions. Transmission electron microscopy, selected area electron diffraction, photoluminescence and UV-Vis absorption spectroscopies have been used to characterize SiNCs. X-ray energy dispersive spectroscopy was used to confirm the presence of erbium. In addition, [24] synthesised SiNCs by co-pyrolysis of disilane where erbium ions derived from erbium amidinate in a dilute He flow at 1000°C. High resolution electron microscopy, selected area electron diffraction, energy dispersive X- ray and PL spectroscopy were used to characterize the samples. These two methods of preparation erbium doped SiNCs provide high concentrations of erbium centered in given SiNCs, thus improvement in the light emission from Er^{3+} has been achieved. Furthermore, they found that the structural and optical properties of SiNCs depend on the location of the erbium ions, where Er^{3+} directly excited by excitons if they dispersed over the Si nanocrystal.

Kik et al. [25] produced SiNCs in silica using silicon ion implantation followed by high temperature annealing. Erbium ions then implanted into SiNCs doped SiO_2 layer. They found that the energy transfer from silicon to erbium ions by the mechanism of electron-hole pair radiative recombination inside SiNCs. In addition, they observed that electron-hole pairs excite erbium ions with efficiency larger than 55% and the maximum number of erbium ions around Si nanocrystals is near unity.

In this letter, we use a new chemical route to mix alkylated silicon nanocrystals (-SiNCs) with Er^{3+} by dispersing Si nanocrystals in deionized water. Alkylated Si nanocrystals then mixed with aqueous erbium tri chloride. Consequently, the chemical changes in alkylated SiNCs, which caused by Er^{3+} have been investigated using X-ray photoemission spectroscopy (XPS) and Fourier transform infrared spectroscopy (FTIR). Meanwhile, the light emission of Er and the optical properties of C_{11}-SiNCs with their mixtures with Er^{3+} have been studied using UV-Vis spectroscopy, Raman spectroscopy and photoluminescence spectroscopy (PL). To the best of our knowledge, there have been no reports on mixing SiNCs with erbium ions by this chemical route.

II. Experimental

A modified version of the method presented by [26] was used to prepare alkyl-capped (11 carbon atoms) SiNCs. This method [27] forms C_{11}-SiNCs with the same optical characteristics with those explained in [26]. Porous silicon was formed by anodic etching of silicon wafer in HF/EtOH. Alkylated silicon nanocrystals were extracted from the porous silicon by a thermal hydrosilation reaction in refluxing toluene. A silicon chip 1×1 cm^2 was cut from a silicon wafer (boron-doped p-Si <100>, 10 Ω cm resistivity, Compart Technology, Peterborough, UK) using a diamond scribe. The silicon chip was then placed in electrochemical cell polytetrafluoroethylene (PTFE) with a diameter of 1 cm and using Viton™ O-ring at the base to seal against the silicon chip. In the cell, a total of 2 mL ethanol and hydrofluoric acid HF (1:1 V/V) solution was added. The electrochemical cell was linked to a power supply and control system (Keithley

2601 and Test Script Builder program) which were set at 400 mA for 5 minutes to etch the silicon and in order to improve the uniformity of the current distribution, a piece of tungsten wire coiled into a loop was used as a counter electrode. After etching, a light orange colour was displayed at the surface of the porous silicon. The chip was cleaned with de-ionized water and dried with nitrogen gas. The dry porous silicon chips also luminesced orange under ultraviolet (UV) light (λ= 365 nm).

Four porous silicon chips were then refluxed in 25 mL of dry toluene solution (previously distilled over Na, Merck) which contained 0.4 mL of the alkene (1-undecene $C_{11}H_{22}$, Merck) for four hours in a Schlenk flask (16 cm in length and 5 cm in diameter). The flask was placed on the magnetic stirrer hot plate linked to a refluxing condenser. During the refluxing time, a clear yellow liquid formed and a flow of nitrogen gas was present in order to keep air out of the Schlenk flask. The boiling point of the solution was around 110°C. Under the UV lamp (λ= 365 nm) an orange color luminescence was emitted by the resulting suspension. After the reflux, the solvent was decanted and transferred to another Schlenk flask. The flask then was placed on the hot plate at low temperature. The flask was also connected to vacuum pump at low pressure in order to evaporate the solvent and unreacted alkenes from this fluorescent solution. The remaining product after the evaporation process was silicon nanocrystals capped with a C_{11} alkyl chain, known as alkylated silicon nanocrystals. In order to dissolve the alkylated silicon nanocrystals from the surface of Schlenk flask, 10 mL of nonpolar solvents i.e. dichloromethane (CH_2Cl_2) was used. This solution was luminescent under UV lamp (λ = 365 nm). Per Si chip, It was estimated that 100 µg of alkyl SiNCs were typically formed [28]. Thus, the concentration of alkylated SiNCs used in the preparation is 0.04 g/L.

Alkyl SiNCs were dissolved then in 200 µL of tetrahydrofuran (THF). Two beakers (each beaker was 15 mL. Fisher Scientific) were filled with 5 mL de-ionized water. (0.007 g, 4 mM, 10 mL) of $ErCl_3.6H_2O$ was added to first beaker and the second beaker was used for blank (i.e. without Er). 100 µL of C_{11}-SiNCs was added to each beaker. Thus, the concentration of C_{11}-SiNCs (0.08 g/L) kept constant during this study. These two beakers were placed on a magnetic stirrer plate for 2 minutes. Two glass vials then were utilized to keep the solutions. The Er/C_{11}-SiNCs mixture was dried in air on a glass slide coverslip for spectroscopic studies.

The chemical characterizations of SiNCs and Er/C_{11}-SiNCs samples were characterized using XPS andFTIR. XPS measurements were carried out at Newcastle University using Kratos Axis Ultra 165 spectrometer with a monochromatic Al K_α X-raysource (photon energy= 1486.6 eV). The pass energy was set at 20.0 eV and 80.0 eV for the survey. A thick film of SiNCs suspension was prepared by a drop cast technique on a gold substrate using a micropipette (Eppendorf) and left overnight to dry in air at room temperature. The binding energy scale of the spectra was calibrated with reference to the Au $4f_{7/2}$ at 84.0 eV[11]. The background was modelled by a Shirley backgroundand the peaks then were fitted using a mixed singlet function [54]. FTIR measurements were carried out at Newcastle University using a Varian 800 Scimitar Series FTIR over the range of 700 - 4000 cm^{-1}. A thick film of the C_{11}-SiNCs that contain erbium ions was prepared by a drop cast method on silicon substrate using a micropipette (Eppendorf) and left overnight to dry in air at room temperature.

The optical properties of alkylated SiNCs, their mixtures with erbium ionand erbium trichloride solution were characterized using UV-Vis spectroscopy (Varian, Cary 100 BIO) at Newcastle University of the wavelength range between 200 to 800 nm using quartz cuvette of 1 cm path length. This measurement was carried out at room temperature. The samples i.e. C_{11}-SiNCs and their mixtures with erbium trichloride was prepared by adding 4 mL of suspension in the quartz cuvette.

Confocal microscope (WiTec confocal Raman microscope model CRM200, Ulm, Germany) at Newcastle University is used to capture Raman spectra and luminescence images of the following samples: SiNCs and their mixtures with erbium ion. An Argon ion laser (Melles-Griot) with output power 35 mW at a wavelength of 488 nm was utilized as the excitation source. The collected light was analyzed by a spectrograph equipped with a CCD detector; a grating of 150 lines mm^{-1} was chosen in order to capture the full spectrum including all Raman and luminescence bands of interest. The scan size of all the experiments was 50 x 50 µm in 100 lines at 100 pixels per line with an integration time of 0.1 s/pixel. Samples of C_{11}-SiNCs and Er/C_{11}-SiNCs were prepared by drop-coating 100 µL of the suspension on a glass slide coverslip using a micropipette (Eppendorf). The samples were air dried over night at room temperature and kept in sealed Petri-dishes to avoid contamination.

The photoluminescence properties of C_{11}-SiNCs and their mixtures with erbium trichloride was carried out in Manchester University, United Kingdom using Fluorolog and cooled InGaAs by Horiba Jobyn Yvon. PL measurements were performed on a thin film of the sample which prepared by the following method. The investigated samples that dispersed in deionized water i.e. C_{11}- SiNCs and Er/C_{11}-SiNCs were prepared by drop-coating 100 µL of each sample on a glass slide coverslip using a micropipette (Eppendorf). The samples were air dried over night at room temperature and kept in sealed Petri-dishes until further analysis.

Two notations were used throughout this work i.e. C_{11}-SiNCs denotes to alkylated silicon nanocrystals alone and Er/C_{11}-SiNCsis erbium mixed alkylated SiNCs.

III. Results & Discussion

Alkylated SiNCs prepared by a modification method from [26] as in [27]. The size, structure and composition of alkylated silicon nanocrystals have been well investigated by our group (Nanoscale Science and Nanotechnology Research Group, Newcastle University, United Kingdom) [27], [29], [30]. Chao et al. [27] reported that these alkylated silicon nanocrystals which refluxed in toluene solution in presence of

1-undecene have a diameter of 2.5 nm, which associate to the silicon core of the nanoparticles.

Fig. 1 (a) shows the Si*2p* spectrum of C_{11}-SiNCs suspension in deionized water dried on gold substrate. The Si*2p* peak has been fitted with a mixed singlet. This figure presents a peak at a binding energy of 101.3 eV. This binding energy of Si*2p* at 101.3 eV is consistent for alkylated SiNCs [27]. This peak assigned to a multicomponent peak that contain different species i.e. bulk silicon, Si-C, Si-H and Si-O [29]. The IR spectrum of the C_{11}-SiNCs [26] confirms the presence of Si-C and Si-O. This peak in this figure is similar to that observed by [27], [29]. They determined a peak for alkylated silicon nanocrystals at 101.6 eV. Obviously, the difference between these two binding energies is 0.3 eV. This difference in the binding energy values are predictable because the thickness of the C_{11}-SiNCs film change in every deposition, thus would impact the degree of charging in the film. The charge effect arises from the long alkyl chain that passivates the surface of SiNCs. Also, the charge effect would likely to be due to the agglomeration of SiNCs as clusters rather than diffuse as individual particles as observed by [27], [29].

Fig. 1 (b) shows the O*1s* core level of C_{11}-SiNCs dried on gold substrate. This peak has been fitted using a mixed singlet. The binding energy at 533.4 eV is assigned to Si-O [31]. Fig. 1 (c) presents a survey spectrum of alkylated silicon nanocrystals. The core lines i.e. Si*2p*, C*1s* and O*1s* are clearly visible in the survey spectrum. Thus, in the film of the investigated sample silicon, carbon and oxygen are present. Some hydrogen atoms may be there in the film but X- ray photoemission spectroscopy cannot detect them [29]. This survey spectrum confirmed also the previous study of IR spectroscopy [26] which exhibits the existence of Si-C and Si-O bonds. The Si-C bonds are anchoring the alkyl chains to dots by covalent bonds while the Si-O bonds arise from the oxidation of unalkyalted Si-H [26]. Altogether, the data suggest that the alkyl chains and sub oxides are present on the surface of silicon nanocrystals.

Fig. 2 presents the FTIR spectrum of Er/C_{11}-SiNCs. It can be seen that there are several IR bands of erbium mixed alkylated silicon nanocrystals sample. The IR peak at 2954 cm^{-1} corresponds to CH_3 stretching mode [26]. The IR peaks that appear at 2921 cm^{-1} and 2854 cm^{-1} are assigned to the methylene C-H asymmetric and symmetric stretching mode, respectively [26]. These three IR bands at 2954 cm^{-1}, 2921 cm^{-1} and 2854 cm^{-1} prove that the long alkyl chains are present in the film of Er/C_{11}-SiNCs. The band at 1459 cm^{-1} corresponds to CH_2 bending mode [26], [32]. The two IR bands at 1259 cm^{-1} and 1220 cm^{-1} are corresponding to Si-CH_2-R bending mode [26], [33]. Broad IR peak occurs at 1053 cm^{-1} as a result of gradual oxidation of the investigated sample which correspond to Si-O-Si symmetric and asymmetric stretching modes [26]. In addition, SiO bending vibration modes appear at the region 700 – 900 cm^{-1} [26]. The IR peaks at 800 cm^{-1} and 615 cm^{-1} are attributed to silanol sites and unalkyalted Si-H bending vibration mode, respectively [26].

The FTIR spectrum of Er/C_{11}-SiNCs in Fig. 2 is similar to that observed by [26]. There is no considerable change in the vibration modes of Er/C_{11}-SiNCs when compared with that of C_{11}-SiNCs as presented in Table I. Thus, these data suggest that the erbium ions (Er^{3+}) do not have effect on the surface of alkylated SiNCs. However, there is no peak determined for erbium trichloride by FTIR spectrum as the erbium does not vibrate in IR range[34]. Thus, XPS is used to determine the surface chemical composition of Er/C_{11}-SiNCs.

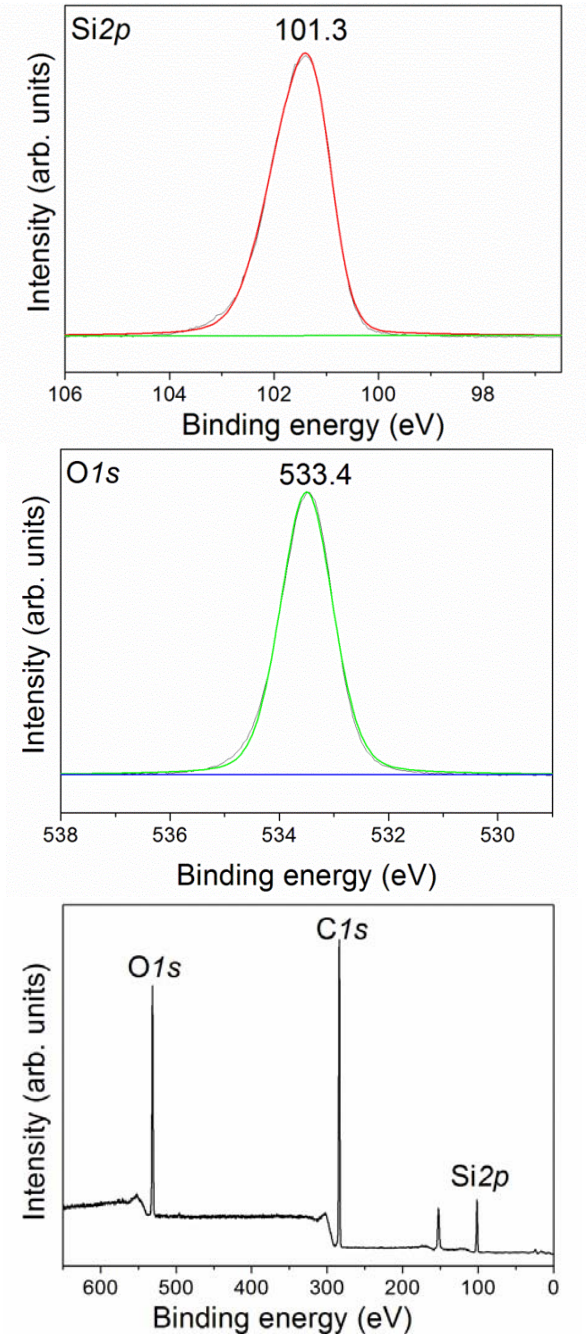

Fig. 1 XPS spectra of C_{11}-SiNCs sample deposit on a gold substrate showing, (a) Si*2p*, (b) O*1s* and (c) survey scan

TABLE I
IR VIBRATIONS BANDS THAT OBSERVED IN FTIR SPECTRA FOR PURE SILICON NANOCRYSTALS AND THEIR MIXTURES WITH ERBIUM IONS

Functional group	Vibration modes	C_{11}-SiNCs (cm^{-1})	Er/C_{11}-SiNCs (cm^{-1})
CH_3	Stretching	2956	2954
CH	Stretching	2926	2921
CH	Stretching	2854	2854
CH_2	Bending	1459	1459
$SiCH_2R$	Bending	1259	1259 & 1220
SiOSi	Stretching	1050	1053
SiO	Bending	700-900	700-900
$Si(CH_3)_3OH$	Bending	800	800
SiH	Bending	615	615

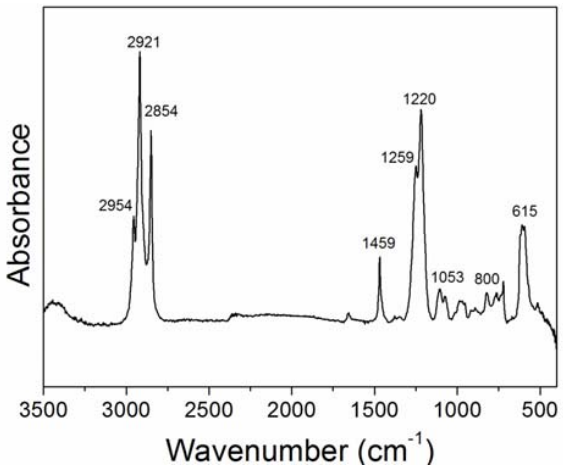

Fig. 2 FTIR spectrum of Er mixed C_{11}-SiNCs deposited on a single crystal silicon wafer

Fig. 3 (a) presents the XPS spectrum of Si*2p* of Er/C_{11}-SiNCs solution dried on gold substrate. This spectrum is similar to that observed by [27]. This peak consists of broad peak with a tail to higher binding energy. This peak has been fitting using mixed singlets. This spectrum is fitted with three peaks with binding energies of 98.6 eV, 102.4 eV and 106.6 eV. They are assigned to different species of Si that are present in Er/C_{11}-SiNCs. The peak at 98.6 eV is assigned to Si [31]. While the peak at 102.4 eV can be attribute to SiO_2, Si_xC_y and Si_xO_y [29], [35], [36]. Furthermore, the higher binding energy component, at 106.6 eV can be associated to saturated peak of silicon[29].

Fig. 3 (b) presents the O*1s* core level spectrum of Er/C_{11}-SiNCs. This spectrum is fitted using mixed singlets into three components i.e. 530.8 eV, 532.6 eV and 533.4 eV. The binding energies at 530.8 eV assigned to Er_2O_3 [35]-[37]. The binding energy at 532.6 eV corresponds to Si_xO_y while the binding energy at 533.4 eV corresponds to SiO_2 [35], [36].

Fig. 3 (c) shows the XPS spectrum of Er*4d* for Er/C_{11}-SiNCs. This peak has also been fitting used mixed singlets. The two peaks constitute a doublet with spin orbit splitting of 2 eV that is consistent with [37]. The binding energy at 168.4 eV and 170.4 eV of Er*4d* assigned to $4d_{5/2}$ and $4d_{3/2}$ of Er_2O_3 [37].

Fig. 3 (d) presents the XPS spectrum of C*1s* for Er/C_{11}-SiNCs. The peak has also been fitting using mixed singlets. This spectrum consist of three peaks i.e. 284.6 eV, 285.8 eV and 288.9 eV which they are correspond to adventitious carbon [38], C-C [39] and Si-C [40], respectively. The FTIR data confirm the presence of Si-C (see Table I).

A survey spectrum of erbium mixed alkylated silicon nanocrystals is plotted in Fig. 3 (e). The core lines of Si*2p*, O*1s*, Er*4d*, and C*1s* are visible and clear which supports the FTIR study (see Fig. 2), that indicate the presence of both Si-O (originate from the oxidation of unalkyalted Si-H) and Si-C (bonded the alkyl chains to the dots). Thus, the XPS data confirm the presence of the components of Si-C and Si-O in binding energy at 102.4 eV. In addition, the data in Fig. 3 (e) show that the silicon nanocrystals are surrounded with a combination of surface SiO_2, Er_2O_3 and alkyl chains.

Comparing the two investigated samples i.e. C_{11}-SiNCs and Er/C_{11}-SiNCs, it can be seen that the core level Si*2p* for alkylated SiNCs shows one multicomponent peak, see Fig. 1 (a), while the core level Si*2p* for erbium mixed alkylated SiNCs presents two peaks, see Fig. 3 (a). It can be explained as result of presence of erbium sesquioxide on the surface of alkylated SiNCs which affect the oxidation states of SiNCs on the surface. Fig. 3 (c) shows the core level Er*4d* for Er/C_{11}-SiNCs, which confirm that the erbium trichloride hydrolysis to Er_2O_3 when mixed with alkylated SiNCs. Meanwhile, Fig. 3 (b) presents O*1s* of Er/C_{11}-SiNCs that prove that Er_2O_3 is present on the surface of C_{11}-SiNCs. This observation can be also interpreted as a result of exposing C_{11}-SiNCs for oxygen and H_2O for long times which increase the amount of Si_xO_y species on the C_{11}-SiNCs surface. These data suggest that the main effect of erbium ions (III) is affecting the oxidation states of alkylated SiNCs.

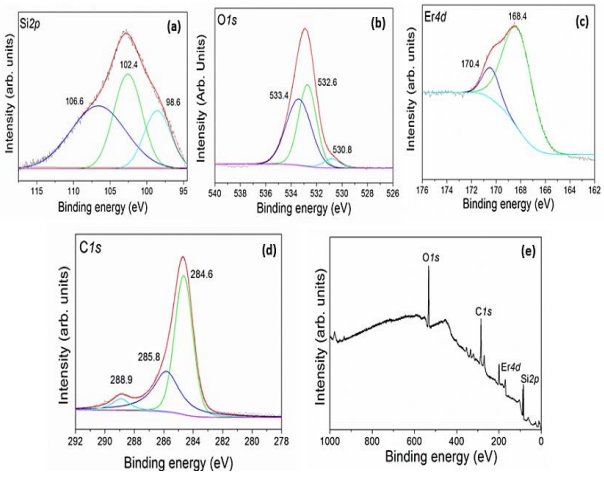

Fig. 3 XPS spectra of Er/C_{11}-SiNCs deposited on gold substrate showing (a) Si*2p*,(b) O*1s*, (c) Er*4d*, (d) C*1s* and (e) survey scan

Fig. 4 shows the absorption spectra of alkylated SiNCs dispersed in deionized water and erbium mixed C_{11}-SiNCs that dispersed in deionized water in the wavelength range from 250 nm to 800 nm. It can be seen that both absorption spectra

present a broad absorption tail with a steep rise feature at around 350 nm which can be assigned to the direct band gap transition (ca. 3.4 eV in bulk silicon). It is known that bulk silicon exhibits direct band gap of 3.4 eV and an indirect band gap of 1.1 eV [26]. Therefore, there is a rapid increase in the absorbance with decreasing the wavelength from the wavelength of 600 nm (2.06 eV) that presents the absorption band edge of the indirect band gap of SiNCs [26], [41], [42]. The result shows the absorption increases as the direct gap is approached as observed by [26]. Fig. 4 indicates also that the presence of erbium ions with C_{11}-SiNCs does not change the absorption spectra of silicon nanocrystals. These absorption spectra of Er/C_{11}-SiNCsis similar to those observed by [23] as this manner is constant for silicon nanocrystals due to indirect band gap.

Figs. 5 (a)-(b) display a reflected light image and luminescence image of alkylated SiNCs do not contain erbium trichloride drop cast on glass coverslip. The confocal luminescence images of dried C_{11}-SiNCs present bright features, which are due to the aggregates of C_{11}-SiNCs as shown in Fig. 5 (b). Figs. 5 (c)-(d) present a reflected light image and luminescence image of alkylated SiNCs do contain erbium ions drop cast on glass coverslip. The bright features confirm the presence of clusters of C_{11}-SiNCs, which are associated to Er^{3+}, see Fig. 5 (d). Mainly, the drying process during sample preparation for the microscopy is the original reason for these aggregates (clusters), which determined in Figs. 5 (b), (d) as these clusters were observed by previous works on confocal Raman spectroscopy [27], [43], [44].

These bright regions of the confocal luminescence images were gathered together in order to provide complete average Raman luminescence spectra for C_{11}-SiNCs and Er/C_{11}-SiNCs as presented in Fig. 6. Fig. 6 (a) provides an average Raman spectrum of C_{11}-SiNCs that exhibit the consistent Raman bands of alkylated SiNCs that prepared by this method. The Raman peak at 515 cm^{-1} is assigned to the first order of crystalline SiNCs as this peak constant for SiNCs [27]. This peak is less than the peak of bulk silicon (520 cm^{-1}) due to quantum confinement effect [27]. The feature at 960 cm^{-1} can be attributed to the second order of SiNCs [28]. There is also a broad and large peak with a maximum at 4915 cm^{-1} (642 nm) which attributed to the orange luminescence signal of alkylated SiNCs due to quantum confinement effect [27], [28], [44]. This orange luminescence peak is characteristic for C_{11}-SiNCs that synthesized by this method as observed by our research group several years ago [26], [28], [45]-[47].

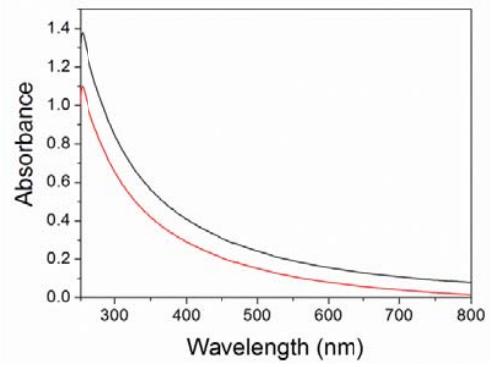

Fig. 4 UV-Vis absorption spectra of C_{11}-SiNCs dispersed in deionized water (black line) and Er/C_{11}- SiNCs dispersed in deionized water (red line)

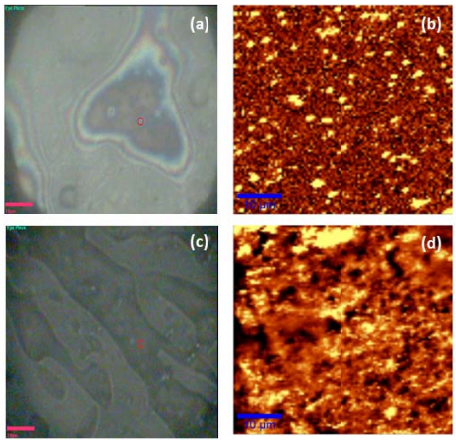

Fig. 5 (a) Reflected light image of C_{11}-SiNCs collected before (b) confocal luminescence spectrum image of dried C_{11}-SiNCs deposited from dichloromethane on the glass coverslip (c) reflected light image of Er/C_{11}-SiNCs collected prior to (d) confocal luminescence spectrum image of dried Er/C_{11}-SiNCs deposited from aqueous solution on the glass coverslip. The laser wavelength was 488 nm and the scale displays the scattered intensity integrated over the Stokes shift range from 200 cm^{-1} to 7000 cm^{-1}, which corresponds to a mixture of Raman signals and the luminescence. The scale bar of the reflected light images (a,c) is 10 µm and the scan size of the luminescence images (b,d) is 50 X 50 µm

Fig. 6 (b) shows the average Raman/luminescence spectrum that observed from erbium mixed alkylated SiNCs that drop coated from deionized water onto glass coverslip. The characteristic large and very broad Raman peak presented in this spectrum with a maximum intensity at around 3960 cm^{-1} (605 nm) can be referred to orange luminescence signals from C_{11}-SiNCs [26]-[28], [44]. It is also should be noted that this peak is a broader than that of alkylated SiNCs. In addition, the position of this peak shifts to a lower wavelength (blue shift) due to the oxidation of alkylated SiNCs in presence of erbium ions. As mentioned The luminescence peak of C_{11}-SiNCs that prepared by the electrochemical method [26] most likely to be affected by the oxidation reaction between the SiNCs and the water. In addition, these oxidations states of alkylated SiNCs (SiO_x) are affected when they mixed with rare earth ion i.e.

Er^{3+} as obtained from the core line Si*2p* in XPS spectrum of Er/C_{11}-SiNCs, see Fig. 3 (a). XPS spectrum shows that the Er/C_{11}-SiQDs have sub oxides on the surface of the nanoparticles. This gives evidence that the blue shift in the luminescence peak of SiNCs in Er/C_{11}-SiNCs arises from states that related with surface oxide. Thus, the surface chemical composition must play an important role in the blue shift of the luminescence of alkylated SiNCs when they mixed with erbium ions. It can be seen also that the typical peak of crystalline Si at 515 cm^{-1} does not appear in presence of erbium trichloride. This observation may be a result of overlap with the Si orange luminescence peak to become one broad peak. Furthermore, the sharp features at around 5145 cm^{-1} likely due to the electronic transitions from $^4F_{9/2}$ to the ground state $^4I_{15/2}$ in erbium ions[48].

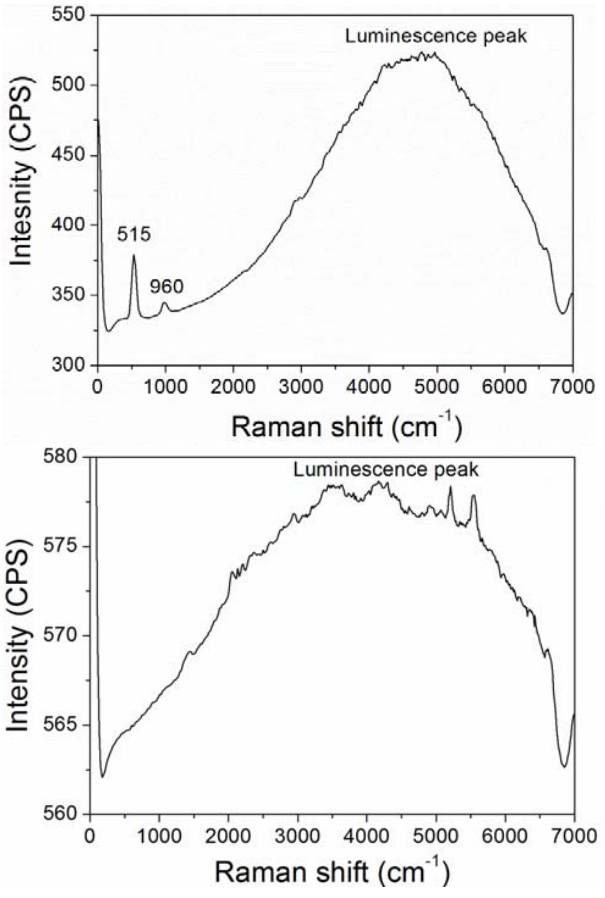

Fig. 6 Average Raman and luminescence spectra of (a) C_{11}-SiNCs drop-coated from dichloromethane solution on glass coverslip (b) Er/C_{11}-SiNCs drop-coated from aqueous solution on glass coverslip. The excitation wavelength = 488 nm line of an argon ion laser was used to excite the luminescence and the spectra was collected using a grating = 150 lines mm^{-1} which provides collection of both Raman and luminescence from alkylated silicon nanocrystals. These spectra are collected as averages from the particles that shown on Figs. 5 (b), (d). The elastically scattered laser light is observed as a higher intensity peak at 0 cm^{-1}

It also can be seen that the intensity of the scattered Raman light from the mixture is higher than that of pure alkylated SiNCs. This enhancement in the intensity can be explained as a result of the presence of erbium ions on the surface of alkyl capped SiNCs that influence the luminescence intensity of Er/C_{11}-SiNCs. Therefore, the typical absorption spectrum of erbium trichloride is carried out in order to interpret this significant improvement in the intensity of the PL peak of Er/C_{11}-SiNCs as shown in Fig. 7. This optical absorption spectrum of erbium trichloride solution shows various bands that correspond to different absorption transitions of erbium ions [48], [49].These electronic transitions bands are listed in Table II. From the typical absorption spectrum of erbium trichloride (Fig. 7), there is an electronic transition peak at 488 nm which attributed to $4F_{7/2}$ [49]. This transition band is corresponding to the laser wavelength at 488 nm of Raman spectroscopy that used to excite the Er/C_{11}-SiNCs sample. Consequently, it is most likely that the laser light has absorbed by Er^{3+} in this transition band and the energy transferred to the C_{11}-SiNCs that reflect the significant enhancement in the intensity of the luminescence band of SiNCs when they mixed with erbium ions (see Fig. 6).

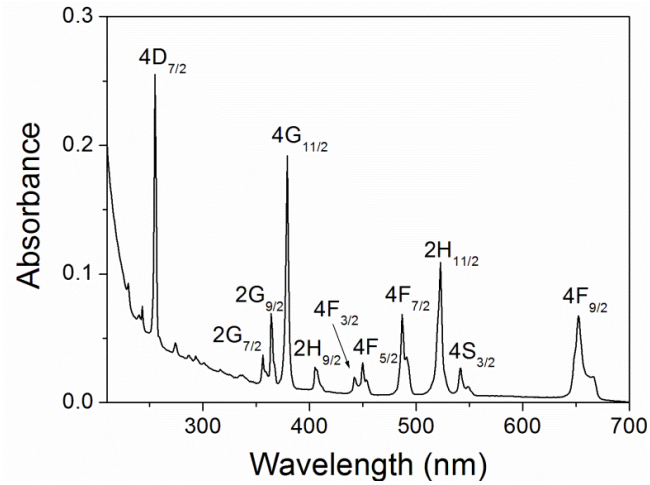

Fig. 7 Absorption spectrum of erbium trichloride dispersed in deionized water

TABLE II
THE EXPERIMENTAL ABSORPTION PEAKS OF ERBIUM ENERGY LEVEL

Energy level	λ_{peak} (nm)
$4F_{9/2}$	652
$4S_{3/2}$	545
$2H_{11/2}$	521
$4F_{7/2}$	488
$4F_{5/2}$	449
$4F_{3/2}$	442
$2H_{9/2}$	405
$4G_{11/2}$	379
$2G_{9/2}$	364
$2G_{7/2}$	356
$4D_{7/2}$	255

The PL emission spectrum of C_{11}-SiNCs drop coated from deionized water onto glass coverslip is presented in Fig. 8 (the excitation wavelength = 400 nm). The sample reveals an orange emission peak at 595 nm (2.1 eV). This peak can be attributed to the band gap transition of alkyl capped SiNCs which is assigned to radiative recombination of excitons inside alkyl capped SiNCs [45]. It is known that the higher energy is required to generate the exciton luminescence in SiNCs which is higher than the band gap energy of bulk silicon due to quantum confinement [25].

XPS spectrum, the absorbance spectrum, Raman spectrum and the emission spectrum of alkyl capped SiNCs that studied in this work are identical with previous work which reported for alkylated SiNCs [26], [27], [29], [30] Thus, these data indicate the successful synthesis of alkyl capped SiNCs.

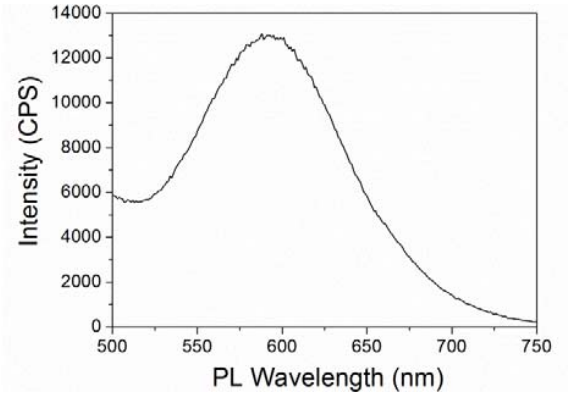

Fig. 8 PL emission spectrum of alkylated SiNCs drop coated from deionized water onto glass coverslip. The excitation wavelength = 400 nm

Fig. 9 indicates the PL emission spectra of erbium mixed alkylated SiNCs which drop coated from deionized water onto glass coverslip. This sample also exhibits the characteristic C_{11}-SiNCs PL band at 595 nm in the region between 500 and 750 nm as seen in Fig. 9 (a) (the excitation wavelength was 400 nm) [45]. The position of this Si peak (595 nm) does not change in the presence of erbium ions; while the intensity of this PL band is considerably higher than the PL intensity band of C_{11}-SiNCs as presented in Fig. 10; where the concentrations of C_{11}-SiNCs are equal in both samples i.e. 0.08 g/L. Fig. 9 (a) presents also PL band at 545 nm which assigned to $4S_{3/2}$ of Er ion [49].

It can be seen also that the peak at 595 nm of erbium mixed alkyl capped SiNCs shows a fourfold increase in the PL emission intensity. This enhancement in the intensity is similar to that observed from Raman spectrum of Er/C_{11}-SiNCs. As mentioned above, this can be explained as a result of the presence of erbium ions on the surface of alkyl capped SiNCs, which influence the luminescence intensity of Er/C_{11}-SiNCs. The absorption spectrum of erbium shows an electronic transition peak at around 405 nm which is assigned to $2H_{9/2}$ [49]. This band is very close to the laser wavelength at 400 nm that used to excite the Er/C_{11}-SiNCs. Hence, it is quite possible that erbium absorbing laser light in this transition band and the energy transferred to the C_{11}-SiNCs from the erbium ion causing a significant enhancement in the intensity of the PL emission band of SiNCs when they mixed with erbium ions.

The PL infrared emission peak at around ≈ 1536 nm in the region between 1400 nm and 1700 nm attributed to the intra-4*f* transition of trivalent erbium (intra-atomic $^4I_{13/2} \rightarrow {}^4I_{15/2}$ transitions of Er^{3+}) [22]and the excitation wavelength was 520 nm, see Fig. 9 (b). It is known that erbium has an important role in optical fiber technology due to its luminescence at around 1535 nm [1]. In addition, the main goal of mixing SiNCs with erbium is to observe the energy transferred from the excited state of Si to the erbium. Thus, Figs. 9 (a), (b) demonstrated that Er/C_{11}-SiNCs sample exhibits simultaneously two PL emission bands corresponding to radiative recombination of electron-hole pairs in alkylated SiNCs (595 nm) and the intra-4*f*transition in Er^{3+} (1536 nm). The latter peak is very weak and the intensity at 1536 nm is around a factor of 1which determines very low PL emission intensity from erbium ions. While, the Si PL peak becomes high in the intensity, as the erbium trichloride exists.

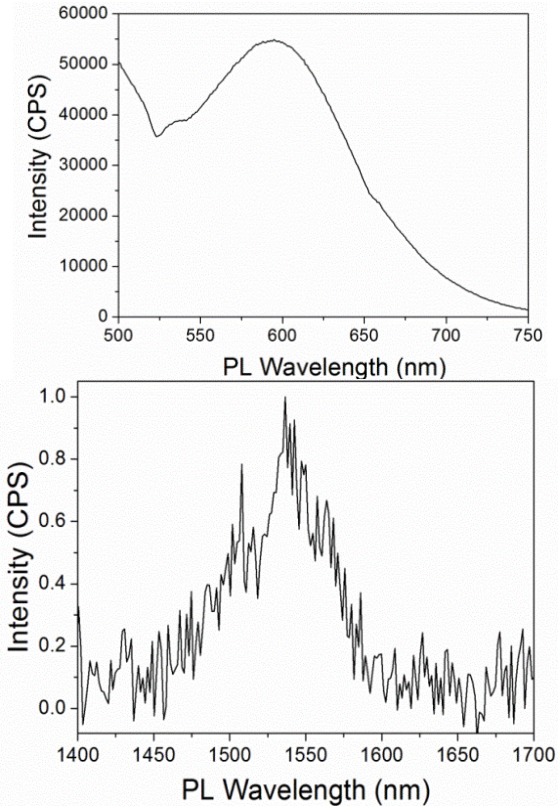

Fig. 9 PL emission spectra of erbium mixed alkylated SiNCs drop coated from deionized water onto glass coverslip showing two different regions (a) 500 – 750 nm and the excitation wavelength was 400 nm (b) 1400 – 1700 nm and the excitation wavelength was 520nm

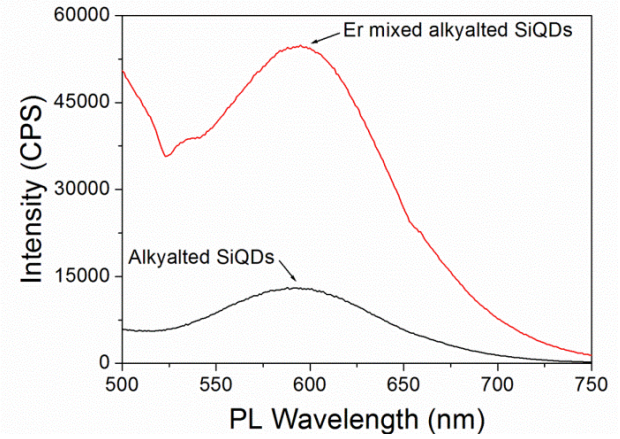

Fig. 10 Comparison PL spectra of C_{11}-SiNCs drop coated from deionized water onto glass coverslip (black line) and Er/C_{11}-SiNCs drop coated from deionized water onto glass coverslip (red line). The excitation wavelength = 400 nm

The lack of the PL Er^{3+} intensity band (1536 nm) can be due to the mixing method that used in this study, which does not growth the PL intensity of erbium in Er/C_{11}-SiNCs mixture, but it causes a significant enhancement in the PL peak of Si nanoparticles. Thus, there is no energy transfer from excited alkylated SiNCs to Er^{3+} as we expected [21], [50] while the energy transfer from erbium ions to alkylated SiNCs. In order to transfer energy from SiNCs to erbium ions, the enhancement of 1536 nm PL emission band should be achieved. Assuming that the energy transferred from alkylated SiNCs to erbium ions (Er^{3+}), Fig. 9 should be interpreted as follow. Basically, the photons are absorbed by alkylated SiNCs and then excitons are generated in the SiNCs [51]. A fraction of recombination energies of the excitons are transferred then to the trivalent erbium. The increased of the total transferred energy to erbium ions depends on the chemical environment. This generates enhancement in the PL intensity peak of erbium (1536 nm) and quenching in the PL intensity peak of Si (595 nm). While, the results from this chemical mixing method which present in Figs. 9 (a), (b) shows growth in the 595 nm PL peak of Si and quenching in the 1536 nm PL band of Er^{3+} which provides a clear evidence that the energy does not transfer from alkylated SiNCs to Er^{3+} as the concentration of SiNCs kept constant in both cases. This can be explained as a result of presence of the erbium in an oxide form i.e. Er_2O_3 as confirmed from XPS results of Er mixed alkylated SiNCs. Thus, the presence of oxides between the erbium and silicon core forbids this energy transfer. Kik et al. [52] and Ji et al. [24] observed that the efficient enhancement in the PL band of erbium at ~1530 nm occur when the Er^{3+} are spaced closely enough to SiNCs in order to allow the energy transfer process.

However, the chemical mixing route that used in this work does not provide efficient PL from erbium ions when they mixed with SiNCs. It is noteworthy that erbium ions have an important emission wavelength centered at about 1535 nm (characteristic for the intra-4*f* transition of Er^{3+}) which correspond to a standard optical telecommunication wavelength [53]. Thus, this study aims to achieve maximum emission intensity from trivalent erbium which generated as a result of the energy transfer from excited silicon nanocrystals to the nearby erbium ion. Regarding to data of Er/C_{11}-SiNCs, this simple chemical mixing of SiNCs and erbium ions leads to transferring energy from erbium ions to SiNCs not as we expected [21], [50] from excited SiNCs to Er^{3+}. Furthermore, this failure to observe optical active erbium may be due to the concentration of erbium that experimentally used which was not sufficient to get efficient Er emission from the samples but affects the photoluminescence of SiNCs considerably. In contrast, previous works [15], [21], [22], [25], [54] have been reported a significant increase in the intensity of the PL emission peak of erbium when the erbium doped silicon nanocrystals by different doping methods such as ion implantation method and sputtering procedure. It was observed that intensity of 1536 nm peak increased dramatically in the presence of silicon nanocrystals and the PL emission peak of silicon nanocrystals is quenched.

However, [21], [15], [54] found that the size of silicon nanocrystals, the chemical environment of erbium doped silicon nanocrystals films and different concentration of erbium ions inside the silicon nanocrystals film affect the PL emission intensities of Si and Er^{3+}. Fujii et al. [21] and Cerqueira et al. [15], [54] found that the intensity of PL peak of erbium ions (1545 nm) increased rapidly with decreasing the size of SiNCs from 3.8 nm to 2.7 nm and from 8 nm to 3 nm, respectively. In addition, they found that the PL intensity of erbium ions increases as the concentration of erbium decreased within the SiNCs. Thus, different intensities of the PL emission bands can be observed depending on the above factors. Thus, it is apparent that the chemical mixing method, chemical environment of the erbium mixed SiNCs and the concentration of erbium trichloride that practically utilized (4 mM) does not transfer energy from SiNCs to Er ion. It is also exert an insignificant effect on the PL efficiency of erbium ions but there is a large effect on the luminescence of SiNCs.

IV. Conclusion

Alkylated silicon nanocrystals (C_{11}-SiNCs) were prepared successfully by galvanostatic etching of p-Si(100) wafers followed by a thermal hydrosilation reaction of 1-undecene in refluxing toluene in order to extract C_{11}-SiNCs from porous silicon. Erbium trichloride was added to alkylated SiNCs using a simple mixing chemical route. To the best of our knowledge, this is the first investigation on mixing SiNCs with erbium ions (III) by this chemical method. However, the main goal of mixing SiNCs with erbium ions is to observe the energy transfer from the excited state of SiNCs to erbium. Erbium is useful because it has a narrow emission spectrum centered at ~ 1500 nm which is a range of interest in optical fiber technology. The erbium trichloride hydrolysis to erbium sesquioxide (Er_2O_3) in Er/C_{11}-SiNCs film, which coat the surface of, alkylated SiNCs. The presence of Er_2O_3 on the surface of C_{11}-SiNCs affects the oxidation state of alkylated

SiNCs on the surface as observed by XPS measurement. C_{11}-SiNCs and their mixtures with Er^{3+} were investigated using Raman spectroscopy and photoluminescence (PL). The characteristic broad luminescence peak confirmed the presence of SiNCs. The wavelength of this luminescence signal of SiNCs in aqueous medium in presence of trivalent erbium shifts to a lower wavelength due to the formation of oxides which would cause a blue shift to higher energy based on the quantum confinement effect. This suggests that the blue shift arises from states that related to the surface oxide on SiNCs. Thus, the surface chemical composition must play an important role in the blue shift of the luminescence of SiNCs when they mixed with erbium ions. This data suggests that the origin of the luminescence from C_{11}-SiNCs could be attributed to direct band gap transitions in SiNCs and to radiative recombination of excitons through the oxidation surface of SiNCs. In addition, the Er/C_{11}-SiNCs sample shows an orange PL emission peak at around 595 nm originates from Si. Er/C_{11}-SiNCs mixture also exhibits a weak PL emission peak at 1536 nm that originates from the intra-4*f* transition in erbium ions (Er^{3+}). The PL peak of Si in Er/C_{11}-SiNCs mixtureis increased in the intensity up to three times as compared to pure C_{11}-SiNCs. The collected data suggest that this chemical mixing route leads instead to a transfer of energy from erbium ions to SiNCs.

ACKNOWLEDGMENT

We would like to thank Taif University and the Ministry of Higher Education, Saudi Arabia for generous support and providing funding.

REFERENCES

[1] S.K. Ray, S. Maikap, W. Banerjee, S. Das, Nanocrystals for silicon-based light-emitting and memory devices, J. Phys. D-Appl. Phys., 46 (2013).
[2] A. Polman, Erbium implanted thin film photonic materials, Journal of Applied Physics, 82 (1997) 1-39.
[3] A.J. Kenyon, Erbium in silicon, Semicond. Sci. Technol., 20 (2005) R65-R84.
[4] O. Savchyn, P.G. Kik, R.M. Todi, K.R. Coffey, Effect of hydrogen passivation on luminescence-center-mediated Er excitation in Si-rich with and without Si nanocrystals, Physical Review B, 77 (2008) 205438.
[5] H. Steinkemper, S. Fischer, M. Hermle, J.C. Goldschmidt, Stark level analysis of the spectral line shape of electronic transitions in rare earth ions embedded in host crystals, New Journal of Physics, 15 (2013) 053033.
[6] P.W. Atkins, V. Walters, J. De Paula, Physical Chemistry, Macmillan Higher Education, 2006.
[7] R.J. Kashtiban, U. Bangert, I.F. Crowe, M. Halsall, A.J. Harvey, M. Gass, Study of erbium doped silicon nanocrystals in silica, in: R.T. Baker (Ed.) Electron Microscopy and Analysis Group Conference 2009, Iop Publishing Ltd, Bristol, 2010.
[8] L.B. Xu, L. Jin, D.S. Li, D.R. Yang, Sensitization of Er3+ ions in silicon rich oxynitride films: effect of thermal treatments, Opt. Express, 22 (2014) 13022-13028.
[9] L.B. Xu, D.S. Li, L. Jin, L.L. Xiang, F. Wang, D.R. Yang, D.L. Que, Evolution of the sensitized Er3+ emission by silicon nanoclusters and luminescence centers in silicon-rich silica, Nanoscale Res. Lett., 9 (2014).
[10] D.S. Korolev, A.B. Kostyuk, A.I. Belov, A.N. Mikhaylov, Y.A. Dudin, A.I. Bobrov, N.V. Malekhonova, D.A. Pavlov, D.I. Tetelbaum, Influence of the ion synthesis and ion doping regimes on the effect of sensitization of erbium emission by silicon nanoclusters in silicon dioxide films, Phys. Solid State, 55 (2013) 2361-2367.
[11] F. Artizzu, F. Quochi, L. Marchio, E. Sessini, M. Saba, A. Serpe, A. Mura, M.L. Mercuri, G. Bongiovanni, P. Deplano, Fully Efficient Direct Yb-to-Er Energy Transfer at Molecular Level in a Near-Infrared Emitting Heterometallic Trinuclear Quinolinolato Complex, J. Phys. Chem. Lett., 4 (2013) 3062-3066.
[12] H. Ennen, J. Schneider, G. Pomrenke, A. Axmann, 1.54-μm luminescence of erbium-implanted III-V semiconductors and silicon, Applied Physics Letters, 43 (1983) 943-945.
[13] H. Ennen, G. Pomrenke, A. Axmann, K. Eisele, W. Haydl, J. Schneider, 1.54-μm electroluminescence of erbium-doped silicon grown by molecular beam epitaxy, Applied Physics Letters, 46 (1985) 381-383.
[14] J.M. Ramirez, F.F. Lupi, Y. Berencen, A. Anopchenko, J.P. Colonna, O. Jambois, J.M. Fedeli, L. Pavesi, N. Prtljaga, P. Rivallin, A. Tengattini, D. Navarro-Urrios, B. Garrido, Er-doped light emitting slot waveguides monolithically integrated in a silicon photonic chip, Nanotechnology, 24 (2013).
[15] M.F. Cerqueira, M. Losurdo, M. Stepikhova, P. Alpuim, G. Andres, A. Kozanecki, M.J. Soares, M. Peres, Photoluminescence of nc-Si:Er thin films obtained by physical and chemical vapour deposition techniques: The effects of microstructure and chemical composition, Thin Solid Films, 517 (2009) 5808-5812.
[16] M.F. Cerqueira, T. Monteiro, M.J. Soares, A. Kozanecki, P. Alpuim, E. Alves, Erbium doped nanocrystalline silicon thin films produced by RF sputtering - annealing effect on the Er emission, physica status solidi (c), 7 (2010) 683-687.
[17] B. Garrido, C. García, P. Pellegrino, D. Navarro-Urrios, N. Daldosso, L. Pavesi, F. Gourbilleau, R. Rizk, Distance dependent interaction as the limiting factor for Si nanocluster to Er energy transfer in silica, Applied Physics Letters, 89 (2006) 163103.
[18] S.A. Denisov, S.A. Matveev, V.Y. Chalkov, V.G. Shengurov, Y.N. Drozdov, M.V. Stepikhova, D.V. Shengurov, Z.F. Krasilnik, Si1-x Ge (x) /Si heterostructures grown by molecular-beam epitaxy on silicon-on-sapphire substrates, Semiconductors, 48 (2014) 402-405.
[19] H. Omar, N.K. Sabri, A. Radzi, M. Rusop, S. Abdullah, N.I. Ikhsan, Optical Characterization of Porous Silicon (PS) doped Erbium (Er) using Photoluminescence Spectroscopy, in: M.H. Mamat, Z. Khusaimi, S.A. Bakar, A.M. Nor, T. Soga, M.R. Mahmood (Eds.) Nanoscience, Nanotechnology and Nanoengineering, Trans Tech Publications Ltd, Stafa-Zurich, 2014, pp. 617-621.
[20] R.J. Kashtiban, U. Bangert, I.F. Crowe, M. Halsall, A.J. Harvey, M. Gass, Study of erbium doped silicon nanocrystals in silica, Journal of Physics: Conference Series, 241 (2010) 012097.
[21] M. Fujii, M. Yoshida, S. Hayashi, K. Yamamoto, Photoluminescence from SiO2 films containing Si nanocrystals and Er: Effects of nanocrystalline size on the photoluminescence efficiency of Er3+, Journal of Applied Physics, 84 (1998) 4525-4531.
[22] M. Fujii, M. Yoshida, Y. Kanzawa, S. Hayashi, K. Yamamoto, 1.54 mu m photoluminescence of Er3+ doped into SiO2 films containing Si nanocrystals: Evidence for energy transfer from Si nanocrystals to Er3+, Applied Physics Letters, 71 (1997) 1198-1200.
[23] J. St. John, J.L. Coffer, Y. Chen, R.F. Pinizzotto, Synthesis and Characterization of Discrete Luminescent Erbium Doped Silicon Nanocrystals, Journal of the American Chemical Society, 121 (1999) 1888-1892.
[24] J. Ji, R.A. Senter, L.R. Tessler, D. Back, C.H. Winter, J.L. Coffer, Rare earth doped silicon nanocrystals derived from an erbium amidinate precursor, Nanotechnology, 15 (2004) 643.
[25] P.G. Kik, M.L. Brongersma, A. Polman, Strong exciton-erbium coupling in Si nanocrystal-doped SiO2, Applied Physics Letters, 76 (2000) 2325-2327.
[26] L.H. Lie, M. Duerdin, E.M. Tuite, A. Houlton, B.R. Horrocks, Preparation and characterisation of luminescent alkylated-silicon quantum dots, Journal of Electroanalytical Chemistry, 538–539 (2002) 183-190.
[27] Y. Chao, L. Šiller, S. Krishnamurthy, P.R. Coxon, U. Bangert, M. Gass, L. Kjeldgaard, S.N. Patole, L.H. Lie, N. O'Farrell, T.A. Alsop, A. Houlton, B.R. Horrocks, Evaporation and deposition of alkyl-capped silicon nanocrystals in ultrahigh vacuum, Nat Nano, 2 (2007) 486-489.
[28] F.M. Dickinson, T.A. Alsop, N. Al-Sharif, C.E.M. Berger, H.K. Datta, L. Šiller, Y. Chao, E.M. Tuite, A. Houlton, B.R. Horrocks, Dispersions of alkyl-capped silicon nanocrystals in aqueous media: photoluminescence and ageing, Analyst, 133 (2008) 1573-1580.
[29] Y. Chao, S. Krishnamurthy, M. Montalti, L.H. Lie, A. Houlton, B.R. Horrocks, L. Kjeldgaard, V.R. Dhanak, M.R.C. Hunt, L. Šiller, Reactions and luminescence in passivated Si nanocrystallites induced by

vacuum ultraviolet and soft-x-ray photons, Journal of Applied Physics, 98 (2005) 044316.
[30] L. Šiller, S. Krishnamurthy, L. Kjeldgaard, B.R. Horrocks, Y. Chao, A. Houlton, A.K. Chakraborty, M.R.C. Hunt, Core and valence exciton formation in x-ray absorption, x-ray emission and x-ray excited optical luminescence from passivated Si nanocrystals at the Si L 2,3 edge, Journal of Physics: Condensed Matter, 21 (2009) 095005.
[31] Y. Hijikata, H. Yaguchi, M. Yoshikawa, S. Yoshida, Composition analysis of SiO2/SiC interfaces by electron spectroscopic measurements using slope-shaped oxide films, Applied Surface Science, 184 (2001) 161-166.
[32] T.J. Pinnavaia, A. Sayari, Nanoporous Materials II, Elsevier Science, 2000.
[33] L.J. Bellamy, The Infra-red Spectra of Complex Molecules, Chapman and Hall, 1975.
[34] B.C. Smith, Fundamentals of Fourier Transform Infrared Spectroscopy, Taylor & Francis, 1995.
[35] M. Losurdo, M.M. Giangregorio, G. Bruno, D. Yang, E.A. Irene, A.A. Suvorova, M. Saunders, Er2O3 as a high-K dielectric candidate, Applied Physics Letters, 91 (2007) 091914.
[36] M. Losurdo, M.M. Giangregorio, P. Capezzuto, G. Bruno, G. Malandrino, I.L. Fragalà, L. Armelao, D. Barreca, E. Tondello, Structural and Optical Properties of Nanocrystalline Er2O3 Thin Films Deposited by a Versatile Low-Pressure MOCVD Approach, J. Electrochem. Soc., 155 (2008) G44-G50.
[37] H.H. Shen, S.M. Peng, X.G. Long, X.S. Zhou, L. Yang, X.T. Zu, The effect of substrate temperature on the oxidation behavior of erbium thick films, Vacuum, 86 (2012) 1097-1101.
[38] G.A. Bhaduri, R. Little, R.B. Khomane, S.U. Lokhande, B.D. Kulkarni, B.G. Mendis, L. Šiller, Green synthesis of silver nanoparticles using sunlight, Journal of Photochemistry and Photobiology A: Chemistry, 258 (2013) 1-9.
[39] S.K. Mishra, A.S. Bhattacharyya, P.K.P. Rupa, L.C. Pathak, XPS Studies on Nanocomposite Si-C-N Coatings Deposited by Magnetron Sputtering, Nanosci. Nanotechnol. Lett., 4 (2012) 352-357.
[40] Y.S. Gu, Y.P. Zhang, X.R. Chang, Z.Z. Tian, N.X. Chen, D.X. Shi, X.F. Zhang, L. Yuan, Synthesis and characterization of C3N4 hard films, Sci. China Ser. A-Math. Phys. Astron., 43 (2000) 185-198.
[41] T. Mohanty, N.C. Mishra, A. Pradhan, D. Kanjilal, Luminescence from Si nanocrystal grown in fused silica using keV and MeV beam, Surface and Coatings Technology, 196 (2005) 34-38.
[42] K.A. Littau, P.J. Szajowski, A.J. Muller, A.R. Kortan, L.E. Brus, A luminescent silicon nanocrystal colloid via a high-temperature aerosol reaction, The Journal of Physical Chemistry, 97 (1993) 1224-1230.
[43] N.A. Harun, M.J. Benning, B.R. Horrocks, D.A. Fulton, Gold nanoparticle-enhanced luminescence of silicon quantum dots co-encapsulated in polymer nanoparticles, Nanoscale, 5 (2013) 3817-3827.
[44] N.A. Harun, B.R. Horrocks, D.A. Fulton, A miniemulsion polymerization technique for encapsulation of silicon quantum dots in polymer nanoparticles, Nanoscale, 3 (2011) 4733-4741.
[45] Y. Chao, A. Houlton, B.R. Horrocks, M.R.C. Hunt, N.R.J. Poolton, J. Yang, L. Siller, Optical luminescence from alkyl-passivated Si nanocrystals under vacuum ultraviolet excitation: Origin and temperature dependence of the blue and orange emissions, Applied Physics Letters, 88 (2006) 263119-263113.
[46] N.A. Harun, Development of New Silicon Quantum Dots–Polymer Composite Nanoparticles via Miniemulsion Polymerization: Synthesis and Characterizations, in: School of Chemistry, Newcastle University, 2013, pp. 156.
[47] K. Zídek, F. Trojánek, P. Malý, L. Ondi, I. Pelant, K. Dohnalová, L. Šiller, R. Little, B.R. Horrocks, Femtosecond luminescence spectroscopy of core states in silicon nanocrystals, Opt. Express, 18 (2010) 25241-25249.
[48] S.V.J. Lakshman, C.K. Jayasankar, OPTICAL-ABSORPTION SPECTRA OF THE TRIPOSITIVE ERBIUM ION IN CERTAIN ACETATE COMPLEXES, Spectroc. Acta Pt. A-Molec. Biomolec. Spectr., 40 (1984) 695-704.
[49] C. Strohhöfer, A. Polman, Absorption and emission spectroscopy in Er3+–Yb3+ doped aluminum oxide waveguides, Optical Materials, 21 (2003) 705-712.
[50] L. Jin, D. Li, L. Xiang, F. Wang, D. Yang, D. Que, Energy transfer from luminescent centers to Er3+ in erbium doped silicon-rich oxide films, Nanoscale Res. Lett., 8 (2013) 1-6.
[51] G. Franzo, V. Vinciguerra, F. Priolo, The excitation mechanism of rare-earth ions in silicon nanocrystals, Appl. Phys. A-Mater. Sci. Process., 69 (1999) 3-12.
[52] P.G. Kik, A. Polman, Exciton–erbium interactions in Si nanocrystal-doped SiO2, Journal of Applied Physics, 88 (2000) 1992-1998.
[53] P.K. Sekhar, A.R. Wilkinson, R.G. Elliman, T.H. Kim, S. Bhansali, Erbium Emission from Nanoengineered Silicon Surface, J. Phys. Chem. C, 112 (2008) 20109-20113.
[54] M.F. Cerqueira, M. Losurdo, T. Monteiro, M. Stepikhova, M.J. Soares, M. Peres, E. Alves, O. Conde, Study of the oxygen role in the photoluminescence of erbium doped nanocrystalline silicon embedded in a silicon amorphous matrix, Journal of Non-Crystalline Solids, 352 (2006) 1148-1151.